FULL PAPER

Dalton
www.rsc.org/dalton

# Coordination chemistry of di-2-pyridylmethane and related bridging ligands with silver(I), copper(II), palladium(II) and zinc(II)

**Peter J. Steel * and Christopher J. Sumby**
*Department of Chemistry, University of Canterbury, Christchurch, New Zealand.*
*E-mail: p.steel@chem.canterbury.ac.nz*

***Received 7th August 2003, Accepted 17th September 2003***
***First published as an Advance Article on the web 7th October 2003***

Di-2-pyridylmethane (**1**) and the bridging ligands 1,1,2,2-tetra(2-pyridyl)ethane (**2**), 1,1,2,2-tetra(2-pyridyl)ethan-2-ol (**3**) and tetra(2-pyridyl)ethene (**4**) chelate to metal atoms with the formation of 6-membered chelate rings. The utility of these ligands in coordination chemistry and as metallosupramolecular synthons was probed by reaction with silver, copper, palladium and zinc salts. On reaction with $AgNO_3$ the model ligand, **1**, formed a 1-D coordination polymer with an unusual bridging mode and with $Cu(NO_3)_2$ underwent oxidation to produce a $Cu_6(L)_4$ (L = **5**, di-2-pyridylmethanediol) complex. The bridging ligands **2** and **4** formed several discrete dinuclear complexes, a [2 + 2]-dimetallomacrocycle and a 1-D coordination polymer. Ligand **3** was demonstrated to be less stable and underwent three different solvolysis reactions to give a range of products that were characterised by X-ray crystallography.

## Introduction

Many nitrogen-containing heterocyclic ligands can function as bridges between two or more transition metal centres and are known to facilitate interactions between the metal atoms through the π-system of the ligand.[1–3] Such multitopic ligands have multiple metal binding sites held in defined geometries by virtue of the ligand structure. The extent of any metal–metal communication is moderated by such factors as the metal–metal distance, the degree of conjugation between the metal centres and the properties of the ligand.[2] In addition to affecting the photochemical, photophysical and electrochemical properties of multinuclear transition metal complexes, bridging ligands have been extensively used as building blocks for the construction of large metallosupramolecular aggregates with well-defined structures.[4] The combination of the structural and functional properties of bridging ligands have led to interesting advances in the areas of multi-electron catalysis, information storage, solar energy conversion, and artificial photosynthesis.[2,5]

Bridging ligands incorporating 2,2′-bipyridine (bpy) subunits coordinate to metal atoms with the formation of stable five-membered chelate rings and have been extensively studied in coordination chemistry.[2,3] Much less studied are the class of ligands shown in Fig. 1 that contain two 2-pyridyl substituents separated by a single atom spacer (X), and which result in the formation of a 6-membered chelate ring.[6] The simplest of these is that in which a methylene group (X = $CH_2$) acts as the spacer. Di-2-pyridylmethane (**1**) has been sparingly used as a ligand.[7,8]

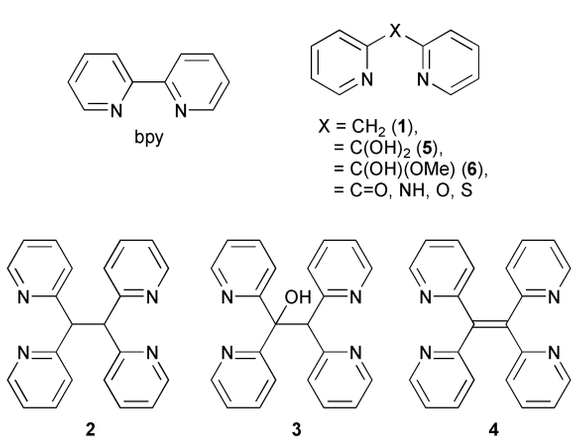


**Fig. 1** The archetypal chelating ligand, bpy, and the ligands investigated in this paper (**1**–**4**). The decomposition products (**5** and **6**) encountered in this study are also shown.

This motif can be extended to three structurally related bridging ligands, 1,1,2,2-tetra(2-pyridyl)ethane (**2**), 1,1,2,2-tetra(2-pyridyl)ethan-2-ol (**3**) and tetra(2-pyridyl)ethene (**4**), which were prepared as described in the literature.[7,9,10] These bridging ligands all contain two di-2-pyridylmethane chelating subunits, and are therefore capable of bridging two metal atoms. Ligand **2** has previously been studied by Canty and Minchin, and a palladium complex of this ligand described.[7,9] An *in situ* preparation of ligand **4**, during the synthesis of a dinuclear copper complex, has also been described,[11] and extended reaction times eventually lead to a copper complex of ligand **3**.[12]

We have recently been involved in a systematic study of ligands capable of forming 6-membered chelate rings and investigations of the structural, electrochemical and photophysical properties of their complexes. Previously, we have reported complexes of these ligands (**1**, **2** and **4**) with octahedral ruthenium centres and described the visible absorption spectroscopy and electrochemistry of those complexes.[10] We also reported crystal structures of mononuclear bis(2,2′-bipyridine) ruthenium complexes of ligands **2** and **4**,[10] but found these ligands to be curiously resistant to forming binuclear complexes. In this paper we report a study of the synthesis and structural chemistry of multinuclear complexes of these ligands with a selection of transition metals.

## Experimental

### General

The ligands investigated in this work, **1**, **2**, **3** and **4**, were prepared by literature procedures.[7,9,10] NMR spectra were recorded on either a Varian 500 MHz or Varian 300 MHz NMR spectrometer. Melting points were performed on an Electrothermal melting point apparatus and are uncorrected. Elemental analyses were performed by the Campbell Microanalytical Laboratory at the University of Otago.

### Preparations

**Complexes of 1.** *[Ag(1)$NO_3$] (7).* Ligand **1** (10.0 mg, 0.059 mmol) and $AgNO_3$ (10.2 mg, 0.060 mmol) were both dissolved in methanol and the two solutions mixed. Slow evaporation gave colourless crystals, suitable for X-ray crystallography. Yield 12.6 mg (63%); mp 160–161 °C (decomp.). Analysis: calc. for $C_{11}H_{10}N_3O_3Ag$ C 38.85, H 2.96, N 12.36; found C 39.10, H 2.83, N 12.37%.

DOI: 10.1039/b309479k

*[Ag(**1**)]$BF_4$ (**8**).* To a methanol solution of **1** (10.0 mg, 0.059 mmol) was added $AgBF_4$ (11.5 mg, 0.059 mmol) dissolved in methanol. Slow evaporation gave a colourless crystalline solid. Yield 12.4 mg (58%); mp 115 °C (decomp.). Analysis: calc. for $C_{11}H_{10}BN_2F_4Ag$ C 36.21, H 2.76, N 7.68; found C 36.63, H 2.56, N 7.64%.

*[Ag(**1**)$_2$]$PF_6$·2$H_2O$ (**9**·2$H_2O$).* Ligand **1** (10.0 mg, 0.059 mmol) dissolved in methanol was combined with a methanol solution of $AgPF_6$ (15.0 mg, 0.059 mmol). A white precipitate formed after two days. Yield 11.1 mg (60%); mp 170 °C (decomp.). Analysis: calc. for $C_{22}H_{24}N_4O_2F_6PAg$ C 41.99, H 3.84, N 8.90; found C 42.32, H 3.52, N 8.52%.

*[Zn(**1**)($NO_3$)$_2$] (**10**).* Both **1** (10.0 mg, 0.059 mmol) and $Zn(NO_3)_2$·6$H_2O$ (17.5 mg, 0.059 mmol) were dissolved in methanol, mixed and the resulting solution slowly evaporated to dryness. The residue was recrystallised by vapour diffusion of diethyl ether into an acetonitrile solution of the complex giving a colourless crystalline solid. Yield 10.1 mg (48%); mp >192 °C (decomp.). Analysis: calc. for $C_{11}H_{10}N_4O_6Zn$ C 36.74, H 2.80, N 15.58; found C 36.89, H 2.71, N 15.66%.

*[Cu$_6$(**5** − H)$_2$(**5** − 2H)$_2$($NO_3$)$_6$]·8$CH_3CN$ (**11**·8$CH_3CN$).* $Cu(NO_3)_2$·3$H_2O$ (14.2 mg, 0.059 mmol) dissolved in methanol was added to a methanol solution of **1** (10.0 mg, 0.059 mmol). Evaporation of the solution gave a blue oil that was crystallised, by vapour diffusion of diethyl ether into an acetonitrile solution of the complex, to give X-ray quality crystals. Yield 16.3 mg (63%); mp 110–112 °C. Analysis: calc. for $C_{60}H_{58}N_{22}O_{26}Cu_6$ C 38.34, H 3.10, N 16.35, found C 40.60, H 3.25, N 15.97%.

**Complexes of 2.** *[Ag(**2**)$NO_3$] (**12**).* Both **2** (10.2 mg, 0.030 mmol) and $AgNO_3$ (10.1 mg, 0.060 mmol) were dissolved in hot acetonitrile, the solutions mixed and allowed to cool overnight. Small colourless crystals precipitated that were suitable for X-ray crystallography. Yield 14 mg (92%); mp 274 °C (decomp.). Analysis: calc. for $C_{22}H_{18}N_5O_3Ag$ C 51.99, H 3.57, N 13.78; found C 51.42, H 3.47, N 13.54%.

*[Ag$_2$(**2**)$_2$]($BF_4$)$_2$ (**13**).* Ligand **2** (10 mg, 0.030 mmol) was dissolved in methanol and $AgBF_4$ (13 mg, 0.067 mmol) was dissolved in hot acetonitrile, the solutions were mixed together and left to slowly evaporate. Yield 15.6 mg (80%); mp >181 °C (decomp.). Analysis: calc. for $C_{44}H_{36}B_3N_8F_{12}Ag_3$·2$H_2O$ C 40.75, H 3.11, N 8.64; found C 40.68, H 2.97, N 8.77%. The above precipitate was recrystallised by vapour diffusion of diethyl ether into acetonitrile to provide colourless crystals of a [2 + 2] dimer.

*[Cu$_2$(**2**)($NO_3$)$_4$] (**14**).* Both **2** (10.6 mg, 0.031 mmol) and $Cu(NO_3)_2$·3$H_2O$ (16.0 mg, 0.066 mmol) were dissolved in methanol, mixed and the resulting solution allowed to slowly evaporate. Dark blue crystals formed that were suitable for X-ray crystallography. Yield 13.0 mg (59%); mp 278 °C (decomp.). Analysis: calc. for $C_{22}H_{18}N_8O_{12}Cu_2$ C 37.03, H 2.54, N 15.70; found C 36.82, H 2.69, N 15.42%.

*[Pd$_2$(**2**)$Cl_4$] (**15**).* $PdCl_2$ (11.5 mg, 0.065 mmol) was dissolved in 2 mL of 2 M HCl and added slowly to a hot methanolic solution of **2** (10.0 mg, 0.030 mmol). The resulting solution turned yellow and a fine yellow solid precipitated. This was collected by filtration and dried *in vacuo*. Yield 12.8 mg (63%); mp > 310 °C (decomp.). Analysis: calc. for $C_{22}H_{18}N_4Cl_4Pd_2$ C 38.13, H 2.62, N 8.08, Cl 20.46; found C 37.80, H 2.85, N 7.49, Cl 20.26%. The complex was insoluble in common NMR solvents.

*[Zn$_2$(**2**)($OAc$)$_4$]·$H_2O$ (**16**·$H_2O$).* $Zn(OAc)_2$ (13.7 mg, 0.062 mmol) and **2** (10.0 mg, 0.030 mmol), were both dissolved in methanol, the solutions combined and the resulting solution allowed to slowly evaporate. Colourless crystals formed which were suitable for X-ray crystal structural analysis. Yield 13 mg (60%); mp 275 °C (decomp.). Analysis: calc. for $C_{30}H_{30}N_4O_8Zn_2$·$H_2O$ C 49.81, H 4.46, N 7.75; found C 49.66, H 4.11, N 7.65%.

**Complexes of 3.** *[Ag(**1**)$NO_3$]·$H_2O$ (**17**·$H_2O$).* Ligand **3** (10.2 mg, 0.029 mmol) and $AgNO_3$ (10.0 mg, 0.059 mmol) were both dissolved in warm methanol, the solutions mixed and on standing for several days colourless crystals formed. Yield 8.4 mg (88%); mp 171–173 °C (decomp.). Analysis: calc. for $C_{11}H_{10}N_3O_3Ag.H_2O$ C 37.85, H 3.18, N 12.04; C 37.75, H 2.21, N 11.77%. Recrystallisation from methanol gave larger crystals suitable for crystal structure analysis.

*[Pd(**6**)$Cl_2$] (**18**).* $PdCl_2$ (9.6 mg, 0.059 mmol) was dissolved in hot 2 M HCl and added dropwise to a methanol solution of **3** (10.0 mg, 0.028 mmol). Yellow crystals, suitable for X-ray crystallography, formed during slow evaporation of the reaction mixture. Yield 10.3 mg (88%); mp 276 °C (decomp.). Analysis: calc. for $C_{12}H_{12}N_2O_2Cl_2Pd$ C 36.62, H 3.07, N 7.12; found C 36.88, H 2.77, N 7.39%. $^1$H NMR (DMSO-$d_6$) $\delta$ 9.19 (d, 2H, H6), 8.46 (t, 2H, H4), 8.27 (d, 2H, H3), 8.01 (t, 2H, H4), 3.27 (s, 3H, $CH_3$).

*[Cu(**5**)$_2$]($NO_3$)$_2$·x$H_2O$ (**19** x=1; **20** x=2).* Methanol solutions of **3** (10.2 mg, 0.029 mmol) and $Cu(NO_3)_2$·3$H_2O$ (13.7 mg, 0.057 mmol) were mixed and left to slowly evaporate. The blue precipitate that resulted was dissolved in acetonitrile and vapour diffusion of diethyl ether into this solution gave a mixture of blue (**19**) and purple crystals (**20**), which were not separated. Both sets of crystals were suitable for X-ray crystallography. Combined yield: 11.4 mg (66%); mp 246–248 °C (decomp.) (**19**); 270 °C (decomp.) (**20**). Analysis: calc. for $C_{22}H_{20}N_6O_{10}Cu$·$H_2O$ C 43.61, H 2.99, N 13.87; found C 43.96, H 2.90, N 14.17%.

**Complexes of 4.** *[Cu$_2$(**4**)($NO_3$)$_4$]·2$H_2O$ (**21**·2$H_2O$).* Ligand **4** (5.8 mg, 0.017 mmol) and $Cu(NO_3)_2$·3$H_2O$ (8.8 mg, 0.036 mmol) were both dissolved in hot methanol and the solutions combined. During slow evaporation of the methanol reaction mixture, small blue crystals formed that were suitable for X-ray crystallography. Yield 10.5 mg (83%); mp >278 °C (decomp.). Analysis: calc. for $C_{22}H_{16}N_8O_{12}Cu_2$·2$H_2O$ C 35.35, H 2.70, N 14.99; found C 35.42, H 2.80, N 14.71%.

*[Pd$_2$(**4**)$Cl_4$]·1½$H_2O$ (**22**·1½$H_2O$).* $PdCl_2$ (10.5 mg, 0.059 mmol) was dissolved in 2 mL of 2 M HCl and added slowly to a hot methanolic solution of **4** (10.0 mg, 0.030 mmol). The solution turned yellow and a fine yellow solid precipitated immediately. This was collected by filtration and dried *in vacuo*. Yield 12 mg (56%); mp >330 °C. Analysis: calc. for $C_{22}H_{16}N_4Cl_4Pd_2$·1½$H_2O$ C 36.80, H 2.67, N 7.80; found C 36.46, H 2.08, N 7.81%. $^1$H NMR (DMSO-$d_6$) $\delta$ 9.07 (d, 4H, H6), 8.17 (t, 4H, H4), 7.54 (t, 4H, H5), 7.49 (d, 4H, H3).

*[Pd$_2$(**4**)($OAc$)$_4$]·3$H_2O$ (**23**·3$H_2O$).* $Pd(OAc)_2$ (13.5 mg, 0.06 mmol) dissolved in acetone was added to a methanolic solution of **4** (10.1 mg, 0.03 mmol). During slow evaporation of the resulting solution, initially a black precipitate formed that was removed by filtration, followed by yellow crystals that were suitable for X-ray crystallography. Yield 11 mg (44%); mp 235–238 °C. Analysis: calc. for $C_{30}H_{28}N_4O_8Pd_2$·3$H_2O$ C 42.93, H 4.08, N 6.67; found C 43.20, H 4.09, N 6.75%.

*[Zn$_2$(**4**)($OAc$)$_4$] (**24**).* Two colourless solutions of **4** (10.0 mg, 0.03 mmol) and $Zn(OAc)_2$ (12.9 mg, 0.059 mmol) dissolved in methanol were mixed to give a white crystalline precipitate. The precipitate was filtered off and the filtrate allowed to slowly evaporate giving large colourless crystals, suitable for a crystal structure determination. Yield 19 mg (90%); mp >269 °C (decomp.). Analysis: calc. for $C_{30}H_{28}N_4O_8Zn_2$ C 51.23, H 4.01, N 7.97; found C 50.92, H 3.93, N 8.03%.

## X-Ray crystallography

The crystal data, data collection and refinement parameters are given in Tables 1 and 2. Measurements were made with a Siemens CCD area detector using graphite monochromatised Mo-K$\alpha$ ($\lambda$ = 0.71073 Å) radiation. The intensities were

**Table 1** Crystal data and X-ray experimental data for complexes **7**, **11**–**14** and **16**–**20**

| Compound | **7** | **11**·5$CH_3CN$ | **12** | **13** | **14**·2$CH_3OH$ | **16** | **17** | **18** | **19**·$H_2O$ | **20**·2$H_2O$ |
|---|---|---|---|---|---|---|---|---|---|---|
| Empirical formula | $C_{11}H_{10}AgN_3O_3$ | $C_{54}H_{49}Cu_6N_{19}O_{26}$ | $C_{22}H_{18}AgN_5O_3$ | $C_{48}H_{42}Ag_2B_2F_8N_{10}$ | $C_{26}H_{34}Cu_2N_8O_{16}$ | $C_{30}H_{30}N_4O_8Zn_2$ | $C_{11}H_{10}AgN_3O_3$ | $C_{12}H_{12}Cl_2N_2O_2Pd$ | $C_{22}H_{22}CuN_6O_{11}$ | $C_{22}H_{24}CuN_6O_{12}$ |
| $M$ | 340.09 | 1761.36 | 508.28 | 1148.28 | 841.69 | 705.32 | 340.09 | 393.54 | 610.00 | 628.01 |
| $T$/K | 168(2) | 168(2) | 168(2) | 168(2) | 168(2) | 168(2) | 168(2) | 168(2) | 168(2) | 158(2) |
| Crystal system | Monoclinic | Monoclinic | Monoclinic | Monoclinic | Monoclinic | Monoclinic | Monoclinic | Monoclinic | Monoclinic | Monoclinic |
| Space group | $P2/c$ | $P2_1/c$ | $Cc$ | $P2_1/c$ | $C2/c$ | $P2_1/c$ | $P2_1/c$ | $P2_1/n$ | $Cc$ | $P2_1/n$ |
| $a$/Å | 5.477(3) | 14.473(4) | 15.948(6) | 9.225(3) | 27.086(13) | 9.898(3) | 9.478(3) | 9.106(3) | 8.000(2) | 7.538(2) |
| $b$/Å | 8.370(5) | 24.872(7) | 11.544(5) | 15.448(6) | 10.055(5) | 7.975(3) | 14.189(4) | 11.784(5) | 32.264(8) | 12.048(3) |
| $c$/Å | 12.711(7) | 20.202(6) | 13.420(5) | 16.892(6) | 14.324(7) | 18.728(6) | 9.136(3) | 12.625(4) | 9.563(2) | 14.550(4) |
| $\beta$/° | 93.762(10) | 107.596(4) | 121.083(5) | 92.551(5) | 119.938(6) | 96.104(4) | 110.702(4) | 91.509(15) | 97.962(3) | 93.479(4) |
| $V$/Å$^3$ | 581.5(6) | 6932(3) | 2116.0(14) | 2404.8(15) | 3380(3) | 1469.8(8) | 1149.3(6) | 1354.2(9) | 2444.5(10) | 1318.9(6) |
| $Z$ | 2 | 4 | 4 | 2 | 4 | 2 | 4 | 4 | 4 | 2 |
| $D_{calc}$/Mg m$^{-3}$) | 1.942 | 1.688 | 1.596 | 1.586 | 1.654 | 1.594 | 1.966 | 1.930 | 1.657 | 1.581 |
| $\mu$/mm$^{-1}$ | 1.737 | 1.901 | 0.987 | 0.891 | 1.344 | 1.690 | 1.757 | 1.762 | 0.969 | 0.903 |
| $F$(000) | 336 | 3552 | 1024 | 1152 | 1728 | 724 | 672 | 776 | 1252 | 646 |
| Reflections collected | 4893 | 50777 | 13344 | 27747 | 21145 | 18324 | 11743 | 9676 | 15172 | 16121 |
| Independent reflections [$R$(int)] | 1175 [0.0346] | 14005 [0.0397] | 3870 [0.0300] | 4818 [0.0517] | 3438 [0.0318] | 2975 [0.0389] | 2245 [0.0326] | 2761 [0.0268] | 4267 [0.0181] | 2624 [0.0417] |
| Observed reflections [$I>2\sigma(I)$] | 861 | 8660 | 3445 | 2844 | 2812 | 2458 | 1795 | 2233 | 4177 | 2219 |
| Goodness-of-fit on $F^2$ | 0.978 | 0.876 | 0.936 | 0.926 | 1.034 | 1.055 | 1.045 | 1.044 | 1.037 | 1.124 |
| $R_1$ [$I>2\sigma(I)$] | 0.0504 | 0.0293 | 0.0227 | 0.0440 | 0.0256 | 0.0289 | 0.0269 | 0.0311 | 0.0250 | 0.0421 |
| $wR_2$ (all data) | 0.1332 | 0.0615 | 0.0407 | 0.1038 | 0.0682 | 0.0749 | 0.0635 | 0.0716 | 0.0693 | 0.0952 |

**Table 2** Crystal data and X-ray experimental data for complexes **21**, **23** and **24**

| Compound | **21**·4$CH_3OH$ | **23**·6$H_2O$ | **24** |
|---|---|---|---|
| Empirical formula | $C_{26}H_{32}Cu_2N_8O_{16}$ | $C_{30}H_{40}N_4O_{14}Pd_2$ | $C_{30}H_{32}N_4O_{10}Zn_2$ |
| *M* | 839.68 | 893.46 | 739.34 |
| *T*/K | 168(2) | 168(2) | 168(2) |
| Crystal system | Monoclinic | Monoclinic | Triclinic |
| Space group | *C*2/*c* | *C*2/*c* | $P\bar{1}$ |
| *a*/Å | 27.587(16) | 19.644(8) | 8.435(2) |
| *b*/Å | 10.068(6) | 15.938(6) | 8.818(2) |
| *c*/Å | 14.049(8) | 14.847(6) | 10.670(3) |
| *α*/° | 90 | 90 | 78.723(3) |
| *β*/° | 119.649(8) | 125.925(5) | 82.103(3) |
| *γ*/° | 90 | 90 | 88.974(3) |
| *V*/Å$^3$ | 3391(3) | 3764(3) | 771.0(3) |
| *Z* | 4 | 4 | 1 |
| $D_{calc}$/Mg m$^{-3}$) | 1.645 | 1.577 | 1.592 |
| *μ*/mm$^{-1}$ | 1.339 | 1.023 | 1.620 |
| *F*(000) | 1720 | 1808 | 380 |
| Reflections collected | 8673 | 12495 | 9413 |
| Independent reflections [*R*(int)] | 2207 [0.1156] | 3285 [0.0267] | 3050 [0.0192] |
| Observed reflections [$I>2\sigma(I)$] | 1308 | 2908 | 2831 |
| Goodness-of-fit on $F^2$ | 1.076 | 1.079 | 1.081 |
| $R_1$ [$I>2\sigma(I)$] | 0.0594 | 0.0230 | 0.0286 |
| $wR_2$ (all data) | 0.1760 | 0.0634 | 0.0763 |

corrected for Lorentz and polarisation effects and for absorption.[13] The space groups were determined from systematic absences and checked for higher symmetry. The structures were solved by direct methods using SHELXS,[14] and refined on $F^2$ using all data by full-matrix least-squares procedures using SHELXL-97.[15] All non-hydrogen atoms were refined with anisotropic displacement parameters. Hydrogen atoms were included in calculated positions with isotopic displacement parameters 1.2 times the isotropic equivalent of their carrier carbon atoms. The functions minimised were $\Sigma w(F_o^2 - F_c^2)$, with $w = [\sigma^2(F_o^2) + aP^2 + bP]^{-1}$, where $P = [\max(F_o)^2 + 2F_c^2]/3$.

CCDC reference numbers 216634–216646.

See http://www.rsc.org/suppdata/dt/b3/b309479k/ for crystallographic data in CIF or other electronic format.

## Results

### Complex syntheses

The preparations of complexes with $AgNO_3$, $Cu(NO_3)_2$, $Pd(OAc)_2$ and $Zn(X)_2$ (X = $NO_3^-$, $OAc^-$) were generally carried out in either methanol or acetonitrile, to give air stable crystalline solids by simply standing or following slow evaporation of the solvent. The $PdCl_2$ complexes were synthesised in 2 M HCl and, on formation, these precipitated as yellow solids. Microanalysis was used to determine the stoichiometry and where possible, the complexes were studied by $^1$H NMR spectroscopy and X-ray crystallography.

Compound **1** was expected to act primarily as a chelating ligand, as previously encountered in several structurally characterised complexes, and not as a bridging ligand (Scheme 1a). To further study the coordination chemistry of **1** it was reacted with a range of metal salts not previously investigated. Complexes of three different silver salts with both coordinating and non-coordinating anions were studied, as were the copper and zinc nitrate complexes. All these complexes serve as models for the study of complexes of the structurally related bridging ligands, **2**, **3** and **4**.

Reaction of **1** with $AgNO_3$ in a 1 : 1 stoichiometry provided colourless crystals of [Ag(**1**)$NO_3$] (**7**) in 63% yield, which analysed with the anticipated 1 : 1 metal–ligand ratio (Scheme 2). These crystals were suitable for X-ray crystallography and were studied to ascertain whether **1** was functioning as a bridging or chelating ligand. As described below the ligand (**1**) was found to act in a bridging mode in this complex. With a labile metal such as silver, the stoichiometry and reaction conditions can strongly influence the type of structure obtained. To probe the effect the anion has on the structure of the $AgNO_3$ complex, **1** was also reacted in a 1 : 1 stoichiometry with both $AgBF_4$ and $AgPF_6$. The former complex, [Ag(**1**)]$BF_4$ (**8**), has the same metal : ligand ratio, and potentially the same structure as (**7**), while the latter complex, [Ag(**1**)$_2$]($PF_6$)·2$H_2O$ (**9**·2$H_2O$), has an entirely different stoichiometry. These complexes were obtained in 58% and 60% yields, respectively. Unfortunately, no crystals were obtained that were suitable for X-ray crystallography, despite several attempts at recrystallising these complexes. A zinc complex, [Zn(**1**)$(NO_3)_2$] (**10**), was prepared by reacting a 1 : 1 mixture of $Zn(NO_3)_2$ and **1** in methanol and isolated as a colourless solid in 48% yield.

A copper nitrate complex, [$Cu_6$(**5** − H)$_2$(**5** − 2H)$_2$($NO_3$)$_6$]·5$CH_3CN$ (**11**·5$CH_3CN$), was obtained in 63% yield by reaction of $Cu(NO_3)_2$ with **1**, but did not provide satisfactory elemental analysis for the expected 1 : 1 metal–ligand complex. Fortunately, blue crystals were obtained of **11** that partially explained some of the difficulties with the elemental analysis. The ligand,

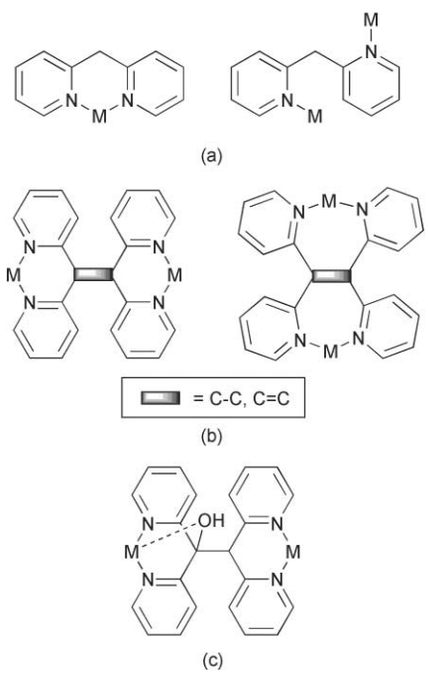


**Scheme 1**

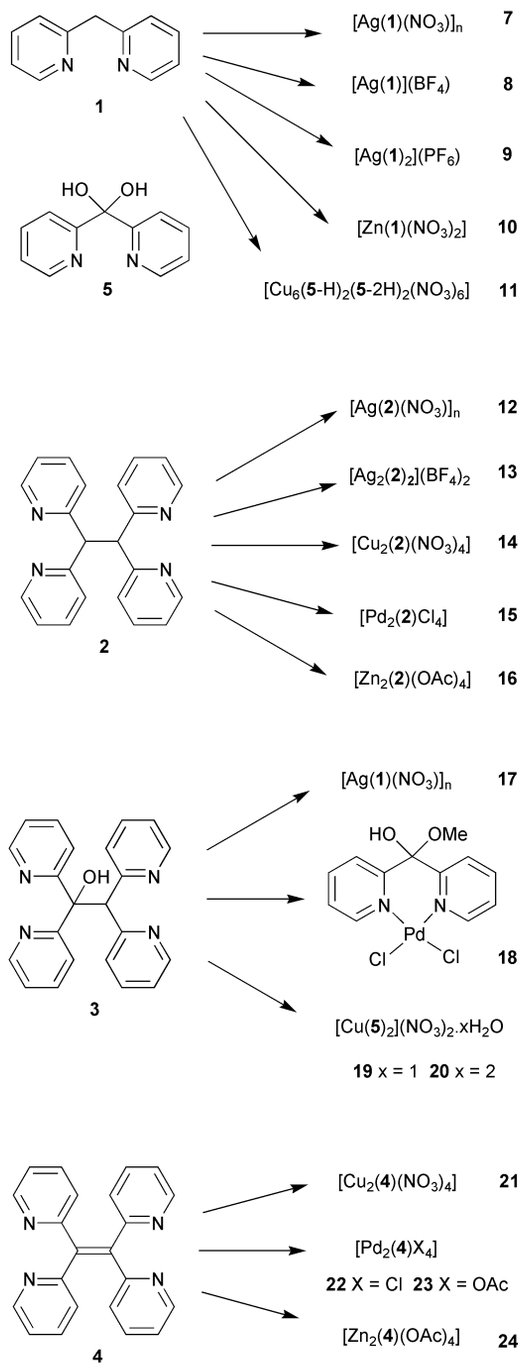


**Scheme 2**

**1**, had undergone oxidation and hydration in the presence of the copper to give di-2-pyridylmethanediol (**5**) (Fig. 1).

Ligand **2** was investigated from a number of standpoints. In contrast to ligand **4**, the ethane ligand has $sp^3$-hybridised carbon atoms in the backbone and dinuclear complexes of this ligand were prepared to provide a comparison for complexes of **4**. Ligand **2** could chelate through the vicinally substituted pyridine rings, forming 7-membered chelate rings. More probably it would be expected to coordinate through the geminally substituted pyridine rings (Scheme 1b), thereby forming 6-membered chelate rings.

$AgNO_3$ was reacted with **2** to give a complex, in 92% yield, with the composition $[Ag(\mathbf{2})NO_3]$ (**12**), as shown by elemental analysis. An X-ray structure determination supported this composition, confirming a 1 : 1 metal–ligand ratio, despite the reaction being carried out with a 2 : 1 stoichiometry. To investigate the effect of the anion on the formation of this silver complex, ligand **2** was reacted with a different silver salt, namely $AgBF_4$. This provided a second silver complex, $[Ag_2(\mathbf{2})_2](BF_4)_2$ (**13**), also with a 1 : 1 metal–ligand ratio.

To demonstrate that ligand **2** could also form discrete dinuclear complexes it was reacted with $Cu(NO_3)_2$ in a metal–ligand ratio of 2 : 1. On standing, dark blue crystals (**14**) were obtained in 59% yield, which analysed with the desired composition of $[Cu_2(\mathbf{2})(NO_3)_4]$ by elemental analysis. To further investigate the coordination chemistry of **2**, it was reacted with $PdCl_2$, but the complex, $[Pd_2(\mathbf{2})Cl_4]$ (**15**), was insoluble in common NMR solvents and could not be examined by NMR spectroscopy. This insolubility also prevented recrystallisation of the complex, which was found to have the desired composition by elemental analysis. Like the corresponding $Pd(OAc)_2$ complex of **2**, which was prepared by Canty and Minchin,[7] the complex would be expected to show a square planar geometry at each palladium centre. A zinc complex was prepared by reaction of $Zn(OAc)_2$ with **2** in a 2 : 1 stoichiometry. Slow evaporation of the methanol reaction mixture gave colourless crystals (**16**), analyzing as $[Zn_2(\mathbf{2})(OAc)_4]\cdot H_2O$, which were suitable for X-ray crystallography.

The ditopic ligand **3** has a number of different potential coordination modes. It possesses two different metal binding domains; one bidentate, like ligand **2**, and the other potentially tridentate with two pyridine nitrogen donors and the oxygen of the alcohol as possible donor atoms (Scheme 1c). To investigate the various coordination modes, several complexes were prepared by reaction of **3** with copper, silver, palladium and ruthenium precursors.

Reaction of **3** with $AgNO_3$ furnished colourless crystals (**17**), with the composition $[Ag(\mathbf{1})NO_3]\cdot H_2O$ determined by microanalysis. X-Ray crystallography was used to confirm that the complex contained **1** and not the original ligand **3**. The crystal structure of this complex, which is discussed below, revealed an interesting feature of **3** concerning its stability. During the synthesis of this complex, **3** undergoes a retro-Knoevenagel reaction to form **1** and di-2-pyridylketone. Aside from the decomposition of **3**, the crystal structure shows **1** again acting as a bridging, as opposed to a chelating, ligand. $^1$H NMR spectroscopy on the bulk sample from the above reaction confirmed the decomposition of **3** and revealed a mixture of two components; one corresponding to **1** and the second to di-2-pyridylketone.

In an effort to prevent the decomposition of **3**, which is stable enough to dehydrate in the preparation of ligand **4**,[10] a palladium complex was prepared under weakly acidic conditions. Yellow crystals were obtained in 88% yield by concentrating the reaction mixture, and studied by X-ray crystallography. The structure of this palladium complex, $[Pd(\mathbf{6})Cl_2]$ (**18**), revealed a further unexpected twist. This time, while the ligand had again decomposed, the structure was that of the hemiacetal of di-2-pyridylketone (**6**) coordinated to a palladium centre.

A similar decomposition was also noted during the synthesis of a copper nitrate complex and in the formation of a ruthenium complex of **3**. Reaction of copper nitrate with **3**, followed by recrystallisation, gave a mixture of blue (**19**) and purple (**20**) crystals. These were shown to have a similar composition by X-ray crystallography, *viz.* $[Cu(\mathbf{5})_2](NO_3)_2\cdot xH_2O$ (where **5** is di-2-pyridylmethanediol and $x = 1$ or 2).

Having investigated the coordination chemistry of ligands **2** and **3**, which have a carbon–carbon single bond connecting the chelating units of the ligand, the focus was shifted to complexes of the conjugated analogue, **4**. Unlike the previous bridging ligands, reacting **4** with a variety of silver salts did not provide any complexes suitable for full characterisation. Reaction of $Cu(NO_3)_2$ with **4** in methanol gave small blue crystals in 83% yield, which analysed as $[Cu_2(\mathbf{4})(NO_3)_4]\cdot 2H_2O$. The structure of this complex (**21**) was determined by X-ray crystallography.

When ligand **4** was reacted with $PdCl_2$ in a 1 : 2 ligand–metal

**Table 3** $^1$H NMR chemical shifts and CIS values for **22**

| | H6 | H5 | H4 | H3 |
|---|---|---|---|---|
| **4** | 8.49 | 7.25 | 7.63 | 7.02 |
| **22** | 9.07 | 7.75 | 8.17 | 7.49 |
| CIS [a] | 0.58 | 0.50 | 0.54 | 0.47 |

[a] $CIS = \delta_{complex} - \delta_{ligand}$.

stoichiometry, the complex that was isolated, $[Pd_2(\mathbf{4})Cl_4]\cdot 1\frac{1}{2}H_2O$ (**22**·$1\frac{1}{2}H_2O$), was soluble in DMSO. A $^1$H NMR spectrum was obtained, consistent with the expected dinuclear complex. The coordination induced shift (CIS) values for this are shown in Table 3, and these show a downfield shift for all the protons of the ligand, as is typical for such complexes. A palladium acetate complex (**23**) was also prepared and crystals of this were obtained by evaporation of the acetone–methanol reaction mixture allowing the X-ray crystal structure of this complex to be determined. These crystals analysed with the composition $[Pd_2(\mathbf{4})(OAc)_4]\cdot 3H_2O$ by elemental analysis. Reaction of **4** with $Zn(OAc)_2$, also in a 1 : 2 stoichiometry, produced a complex (**24**) that analyses as $[Zn_2(\mathbf{4})(OAc)_4]$ by elemental analysis. These crystals were also suitable for crystal structure analysis.

### X-Ray crystallography of complexes of ligand 1

**Structures of $[Ag(1)NO_3]$ (7) and $[Ag(1)NO_3]$ (17).** Two different polymorphs of a 1-D coordination polymer composed of $AgNO_3$ and **1** were prepared by reaction of $AgNO_3$ with either **1** or **3** (which decomposes to give **1** *in situ*). When directly prepared from **1**, colourless crystals of **7**, which crystallises in the monoclinic space group *P*2/*c* with one half of a ligand molecule, half a silver atom and half a nitrate anion in the asymmetric unit, were obtained directly from the reaction mixture. Reaction of **3** with $AgNO_3$ led to decomposition of the ligand as described above, and in contrast to **7**, this second polymorph (**17**) crystallises in the monoclinic space group $P2_1/c$ with the asymmetric unit containing one complete molecule of **1**, one silver atom and one nitrate anion. Complex **17** possesses a slightly different conformation of the ligand and different packing interactions. The coordination mode of ligand **1** in the structures of **7** and **17** involves its unexpected bridging between two metal centres.

A perspective view of the extended structure of complex **7**, shown in Fig. 2 with selected atomic labelling, confirms the complex is a one-dimensional coordination polymer. One two-fold rotation axis passes through the silver nitrate and another through the methylene carbon of the ligand. The geometry of the silver atom is almost linear, but it makes two weak contacts with the oxygen atoms of the weakly coordinating nitrate anion with a Ag–O distance of 2.630(5) Å. A consideration of the packing reveals that there are very weak π–π stacking interactions (3.740(9) Å) between the pyridine rings of adjacent coordination polymers. As noted earlier, there are no previous examples of structurally characterised complexes where di-2-pyridylmethane bridges between two metal centres and therefore, the complexes characterised here are the first examples of such a coordination mode for **1**.

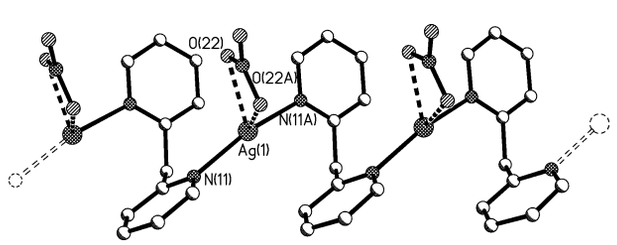


**Fig. 2** A perspective view of the one-dimensional coordination polymer (**7**), formed from silver nitrate and **1**. Selected bond length (Å) and angle (°): Ag(1)–N(11) 2.235(5); N(11A)–Ag(1)–N(11) 162.9(2).

In the polymorph **17** the Ag–N bond lengths and angles about the silver atom are 2.183(2) and 2.184(2) Å with an angle between the two pyridine donors of 164.46(9)°. These bond distances and angles are similar to those found in the previous complex. The silver also makes very weak Ag–O interactions with two different nitrate anions, which act as weak bridges between the polymer chains. The Ag–O distances range from 2.713(3) to 2.908(4) Å. These are considerably longer than the Ag–O bond distances for the polymorph **7**.

**Structure of $[Cu_6(5-H)_2(5-2H)_2(NO_3)_6]\cdot 5CH_3CN$ (11·5$CH_3CN$).** Having observed a bridging mode for **1** in complexes **7** and **17**, another unexpected observation was noted when **1** was reacted with $Cu(NO_3)_2$. Crystals of this complex were obtained by vapour diffusion of diethyl ether into an acetonitrile solution of the complex and studied by X-ray crystallography. This revealed that the original ligand had undergone oxidation, in the presence of the copper ions, to give di-2-pyridylmethanediol (**5**, see Fig. 1) which was incorporated into the complex. The complex (**11**) crystallises in the monoclinic space group $P2_1/c$, with a complete $M_6L_4$ cluster and five acetonitrile molecules in the asymmetric unit. This $M_6L_4$ cluster is constructed from two different $M_2L_2$ components, orientated at 90° relative to each other, and two additional capping copper atoms. The asymmetric unit of the complex, excluding hydrogen atoms and solvate molecules, is shown in Fig. 3.

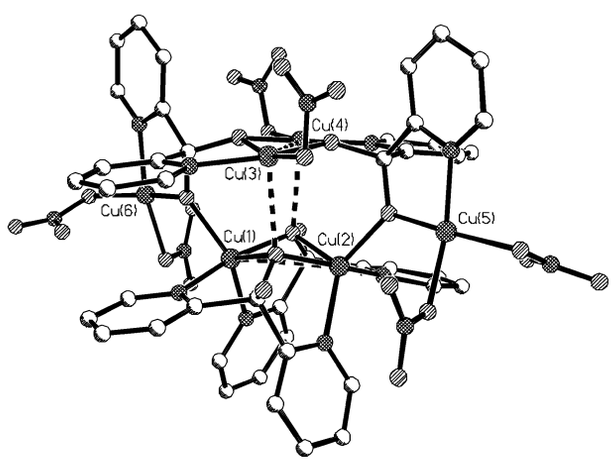


**Fig. 3** The $M_6L_4$ cluster **11**·5$CH_3CN$ formed by reaction of **1** and copper nitrate. Selected metal–metal distances (Å): Cu(1)–Cu(2) 2.928(1), Cu(3)–Cu(4) 3.015(1), Cu(1)–Cu(6) 3.440(1), Cu(2)–Cu(5) 3.471(1).

There are three distinct coordination environments for the copper atoms in this structure. Excluding the copper–copper interaction, Cu(1) and Cu(2) both have trigonal-bipyramidal geometry, with coordination by two pyridine nitrogen atoms and three deprotonated $\mu_2$-bridging oxygen atoms of the ligand. Two of the $\mu_2$-bridging oxygen atoms bridge only across the Cu(1)–Cu(2) dimer, while a third bridges between these copper atoms and one of the capping copper atoms (Cu(5) and Cu(6)). The latter oxygen atoms are two of the links holding the two dimeric units together. The coordination geometry of both Cu(3) and Cu(4) is square-pyramidal when the copper–copper interaction is excluded. In this copper dimer, both copper atoms are coordinated in the basal plane by two $\mu_2$-bridging oxygen atoms, a pyridine nitrogen and a monodentate nitrate anion. The $\mu_2$-bridging oxygen atoms of the other [*i.e.* Cu(1)–Cu(2)] dimer make weak contacts (2.472(6) and 2.476(6) Å) to the axial coordination sites of Cu(3) and Cu(4) (see Fig. 3). Cu(5) and Cu(6) both possess Jahn–Teller distorted octahedral coordination geometries with typical Cu–N and Cu–O bond lengths to the atoms in the square plane. Both copper atoms make two longer axial contacts, with Cu–O distances ranging

between 2.484(6) and 2.559(7) Å, to the second oxygen atoms of the coordinated nitrate anions (bonds not shown in Fig. 3).

The geometry of the $M_2L_2$ dimer between Cu(1) and Cu(2), which adopts a puckered butterfly conformation, is shown in Fig. 4(a), while the other $M_2L_2$ copper dimer, involving Cu(3) and Cu(4), is almost planar (Fig. 4(b)). The metal–metal distances in these two dimers are 2.928(1) and 3.015(1) Å respectively, a value typical for such interactions.[16] These $Cu_2O_2$ squares are part of a larger family of $Cu_2X_2$ squares, where X is a range of monatomic bridges, and have been the subject of an exhaustive review.[16] $Cu_2X_2$ squares like the ones observed here are of interest from a number of perspectives, but in particular in the context of magnetic behaviour of such complexes.[16]

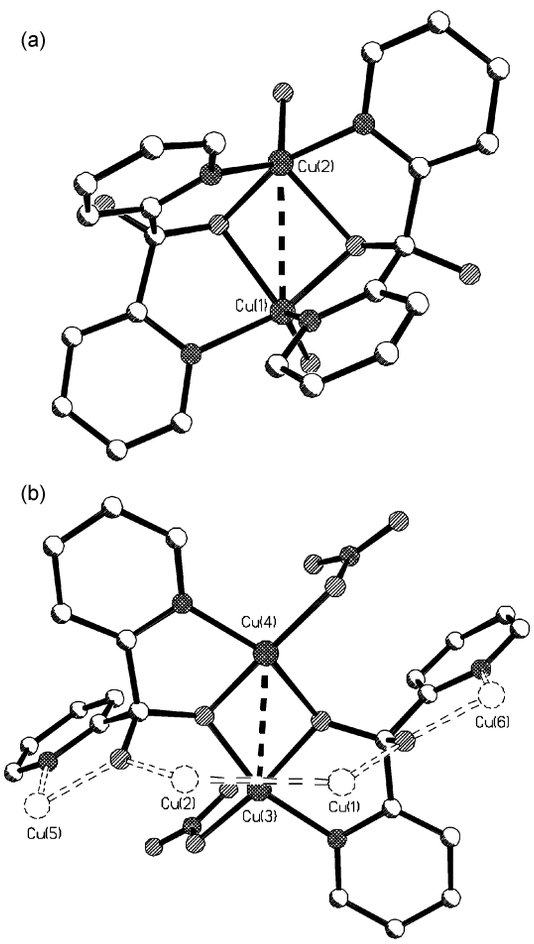


**Fig. 4** A perspective view of (a) the butterfly shaped $M_2L_2$ copper dimer involving Cu(1) and Cu(2) and (b) the planar $M_2L_2$ copper dimer involving Cu(3) and Cu(4) in complex **11**·5$CH_3CN$.

An interesting aspect of this structure, mentioned above, is that **1** has undergone oxidation to produce both the singly and doubly deprotonated forms of di-2-pyridylmethanediol. The two molecules of **5** bridging Cu(1) and Cu(2) are present as the singly deprotonated form, while the two molecules bridging Cu(3) and Cu(4) are doubly deprotonated. Compound **1** is relatively stable in the presence of acids and bases, but has been shown to react with di-2-pyridylketone in the presence of copper ions by other workers.[11] When $Cu(ClO_4)_2$ was reacted with a mixture of di-2-pyridylketone and **1**, the formation of a copper complex of ligand **4** was observed after short periods of reaction at room temperature. Subsequently, after longer reaction times at elevated temperature, the formation of a copper complex of **3** was observed.[12]

## X-Ray crystallography of complexes of ligand 2

**Structure of [Ag(2)$NO_3$] (12).** Elemental analysis had indicated a 1 : 1 silver–ligand ratio for complex **12**, suggesting the possibility of a bridging coordination mode for ligand **2**. The complex crystallises in the monoclinic space group *Cc*, with an asymmetric unit containing one molecule of **2**, a silver atom and a nitrate anion. A perspective view of the extended coordination polymer is shown in Fig. 5 with selected atom labelling and showing that **2** employs all four potential donor atoms in this complex. The geometry of the silver atom is distorted trigonal-bipyramidal, with coordination by four pyridine rings of two crystallographically related ligand molecules and

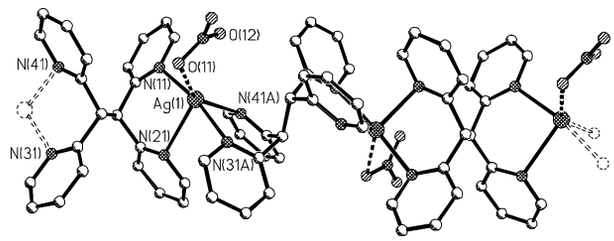


**Fig. 5** A perspective view of the structure of a section of the polymer **12**. Selected bond distances (Å) and angles (°): Ag(1)–N(11) 2.312(4), Ag(1)–N(21) 2.635(3), Ag(1)–N(31A) 2.343(4), Ag(1)–N(41A) 2.469(3), Ag(1)–O(11) 2.671(3); N(11)–Ag(1)–N(31A) 170.04(12), N(11)–Ag(1)–N(41A) 96.59(10), N(31A)–Ag(1)–N(41A) 84.62(10), N(11)–Ag(1)–N(21) 84.44(10), N(31A)–Ag(1)–N(21) 85.92(10), N(41A)–Ag(1)–N(21) 82.44(8).

an oxygen atom of the nitrate anion. The nitrate anion makes another long contact with the silver atom, and hence the geometry could be described as highly distorted octahedral. The silver–nitrogen distances range from 2.312(4)–2.635(3) Å, while the nitrate oxygen atoms are slightly further distant at 2.672(3) and 2.786(3) Å; the latter distance to O(12), represents a very long and weak interaction. The Ag–N bonds to the pyridine nitrogen atoms N(21) and N(41A) in the trigonal plane are longer than the bonds to the nitrogen atoms of the pyridine rings in the axial coordination sites. The silver–silver distance in this complex is 6.835(1) Å.

While the complex demonstrates the potential of **2** for a number of bimetallic complexes, the extended structure of **12** is an interesting one-dimensional coordination polymer. The polymer is helical and extends along the crystallographic *c*-axis of the unit cell. The nitrate anion alternates on opposite sides of the coordination polymer at each silver atom, while the ligand twists by approximately 90° at each repeat. No significant interactions occur between the different coordination polymer chains in the crystal with only weak interactions by the non-coordinated oxygen atom of the nitrate anions with the pyridine hydrogen atoms of adjacent polymer chains.

**Structure of [$Ag_2$(2)$_2$]($BF_4$)$_2$·2$CH_3CN$ (13·2$CH_3CN$).** As was mentioned above, the choice of anion often plays a pivotal role in the solid-state structure of silver complexes and, thus, despite having the same stoichiometry as **12**, an X-ray crystal structure determination was undertaken on complex **13**. This revealed that complex **13** does indeed have a different structure to **12**. It crystallises in the space group $P2_1/c$, with one ligand molecule, one disordered silver atom, a tetrafluoroborate counterion and an acetonitrile solvate molecule in the asymmetric unit. The overall structure of **13** is a [2 + 2]-dimetallomacrocycle, as shown in Fig. 6.

Each silver atom is trigonal-planar with coordination by one pyridine ring of one ligand and chelation by two pyridine rings of the second ligand molecule. The bond distances are 2.302(2) and 2.344(3) Å for the chelating pyridine rings, and slightly shorter (2.266(3) Å) for the monodentate pyridine donor (N(41A)) of the other ligand. The geometry of the silver atom

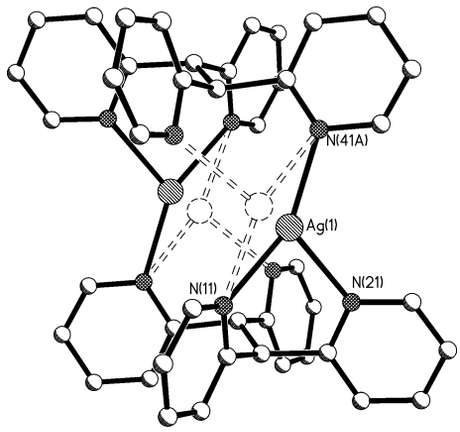


**Fig. 6** A perspective view of complex **13** shows the two positions of the silver atom. The dashed bonds and atoms show the minor component of the structure. Selected bond distances (Å) and angles (°): Ag(1)–N(41A) 2.266(3), Ag(1)–N(11) 2.302(2), Ag(1)–N(21) 2.344(3), N(41A)–Ag(1)–N(11) 150.62(10); N(41A)–Ag(1)–N(21) 122.62(11), N(11)–Ag(1)–N(21) 85.87(10).

is distorted away from trigonal-planar because the angle between the chelating pyridine rings is acute, and consequently, this enlarges the angle between N(11) and N(41A). In each component of the structure one of the pyridine ring nitrogen atoms is not involved in coordination to the silver atoms, and the ligand can therefore be described as hypodentate.

The silver atom is disordered over two sites, as indicated in Fig. 6, with a 7 : 3 ratio of site occupancies. The silver–silver distance in this complex is 3.893(1) Å, and because of the nature of the complex, considerably shorter than that in complex **12**. The discrete [2 + 2]-dimetallomacrocyclic complexes pack in the crystal with no significant interactions between the individual [2 + 2] complexes. There are weak contacts with the tetrafluoroborate anions, which are located in the voids between the [2 + 2]-dimetallomacrocycles.

**Structure of $[Cu_2(2)(NO_3)_4(CH_3OH)_2]\cdot 2CH_3OH$ ($14\cdot 2CH_3OH$).** Complex **14** crystallises in the monoclinic space group $C2/c$, with four molecules of **14** in the unit cell. The asymmetric unit consists of one metal atom, half the bridging ligand, one coordinated methanol molecule, two coordinated nitrate anions and one non-coordinated methanol solvate molecule, with the latter three units each disordered over two sites. A perspective view of **14** is shown in Fig. 7, with the non-coordinated solvate molecules and the disorder of the nitrate anions omitted for clarity. The copper atoms have a square-pyramidal geometry ($\tau$ value of 0.01)[17] with the coordinated methanol solvate molecule occupying the apical coordination position. The Cu–N distances are typical (1.992(2) and 2.000(2) Å), as are the Cu–O bond distances to the monodentate nitrate anions, while the methanol solvate molecule is coordinated at a longer distance of 2.269(2) Å. The copper–copper distance is 6.698(1) Å, similar to that in the previous silver nitrate complex, **12**.

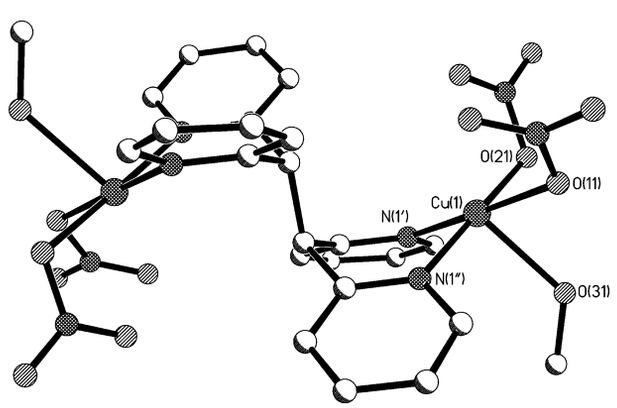


**Fig. 7** A perspective view of the dinuclear copper complex **14**. Selected bond lengths (Å) and angles (°): Cu(1)–N(1′) 1.992(2), Cu(1)–N(1″) 2.000(2), Cu(1)–O(21) 2.006(15), Cu(1)–O(11) 1.967(8), Cu(1)–O(31) 2.269(2); O(11)–Cu(1)–N(1′) 175.0(4), O(11)–Cu(1)–N(1″) 96.7(3), N(1′)–Cu(1)–N(1″) 88.32(7), O(11)–Cu(1)–O(21) 87.3(7), N(1′)–Cu(1)–O(21) 87.7(6), N(1″)–Cu(1)–O(21) 175.6(6), O(11)–Cu(1)–O(31) 78.7(3), N(1′)–Cu(1)–O(31) 99.97(7), N(1″)–Cu(1)–O(31) 96.82(7), O(21)–Cu(1)–O(31) 82.1(5).

**Structure of $[Zn_2(2)(OAc)_4]$ (16).** A second discrete dinuclear complex of ligand **2** was obtained by reaction with zinc acetate. Complex **16** crystallises in the monoclinic space group $P2_1/c$ with $Z = 2$. The asymmetric unit contains one zinc atom, half the bridging ligand and two monodentate acetate anions. The zinc atom has tetrahedral geometry, with chelation by the ligand to give a 6-membered chelate ring, in a boat conformation, characteristic of complexes where this ligand chelates to a metal centre. A perspective view of **16** is shown in Fig. 8, with selected bond lengths and angles given in the caption. The oxygen atoms of the acetate anions are held closer to the zinc, with bond lengths of 1.946(2) and 1.974(2) Å, than the pyridine nitrogen donors (2.094(2) and 2.119(2) Å). The geometry of the zinc atom is distorted away from a strict tetrahedral geometry by the chelation to **2** with the bond angle for N(21)–Zn–N(11) of 89.57(7)°. The zinc–zinc distance in **16** is 6.571(1) Å, a value that is very similar to the corresponding distance in complex **14** (6.698(1) Å).

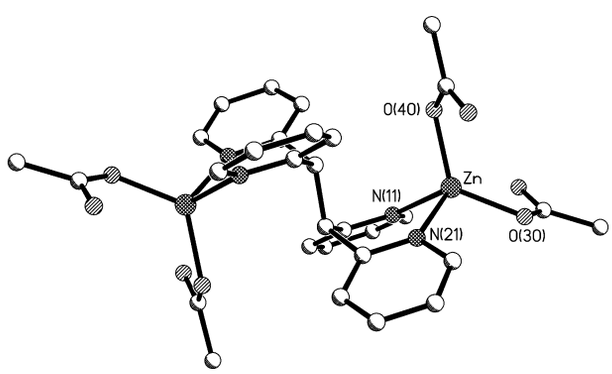


**Fig. 8** A perspective view of complex **16** with the hydrogen atoms omitted for clarity. Selected bond lengths (Å) and angles (°): Zn–N(21) 2.094(2), Zn–N(11) 2.119(2), Zn–O(30) 1.946(2), Zn–O(40) 1.974(2); O(30)–Zn–O(40) 123.91(8), O(30)–Zn–N(21) 98.20(8), O(40)–Zn–N(21) 121.04(7), O(30)–Zn–N(11) 122.66(8), O(40)–Zn–N(11) 97.85(7), N(21)–Zn–N(11) 89.57(7).

### X-Ray crystallography of complexes of ligand 3

**Structure of $[Pd(6)Cl_2]$ (18).** As discovered by X-ray crystallography, during the synthesis of complex **17**, ligand **3** underwent decomposition. Similar behaviour was observed for complex **18**, with the structure of complex **18** shown in Fig. 9. Unfortunately, the acidic conditions of the reaction did not prevent decomposition of **3** as was intended. $^1$H NMR spectroscopy on the bulk sample from this reaction revealed a mixture of two components corresponding to decomposition of the original ligand. Compound **3** probably decomposed to give a mixture of **1** and di-2-pyridylketone, the latter of which, on coordination to a metal atom, is susceptible to nucleophilic attack by methanol.[18]

The palladium atom is square planar with bond lengths and angles typical for such a complex. The oxygen of the methoxy group of the hemiacetal interacts very weakly (2.755(5) Å) with the palladium atom. Complexes of this ligand, **6**, prepared directly by solvolysis of di-2-pyridylketone, have previously been characterised by X-ray crystallography with cobalt,[19]

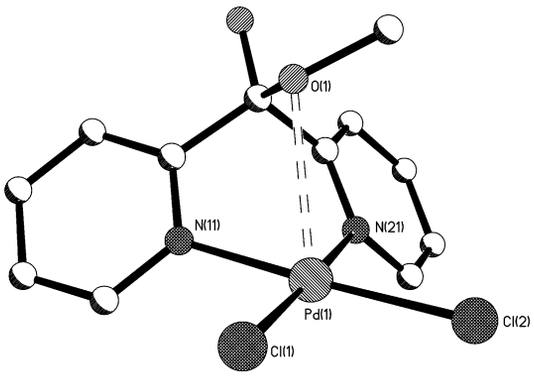


**Fig. 9** A perspective view of the decomposition product, **18**, formed by reacting palladium chloride with **3**. Selected bond lengths (Å) and angles (°): Pd(1)–N(11) 2.028(3), Pd(1)–N(21) 2.044(3), Pd(1)–Cl(2) 2.2891(11), Pd(1)–Cl(1) 2.2953(12); N(11)–Pd(1)–N(21) 86.44(12), N(11)–Pd(1)–Cl(2) 176.91(8), N(21)–Pd(1)–Cl(2) 90.89(9), N(11)–Pd(1)–Cl(1) 91.29(9), N(21)–Pd(1)–Cl(1) 177.74(8), Cl(2)–Pd(1)–Cl(1) 91.37(4).

copper,[18,20] zinc[21] and palladium,[22] the latter in the form of a square planar palladium trifluoroacetate complex. In these complexes the interaction with the methoxy oxygen is more significant with M–O distances between 2.371 Å (M = Zn) and 2.614 Å (M = Cu), reflective of the fact that palladium forms very stable square planar complexes. No unusually short intermolecular contacts are present in the structure.

**Crystal structures of $[Cu(5)_2](NO_3)_2 \cdot xH_2O$ (19 $x = 1$; 20 $x = 2$).** Two different crystalline products were isolated from the reaction of copper nitrate with **3**; blue crystals (**19**) and purple crystals (**20**). When crystal structure determinations were undertaken on both sets of crystals it was discovered that the crystals had almost identical compositions. In both cases the ligand, **3**, had been hydrolysed to di-2-pyridylmethanediol (**5**) in the presence of the copper and a Jahn–Teller distorted octahedral complex, $[Cu(\mathbf{5})_2](NO_3)_2 \cdot xH_2O$, of this decomposition product had formed. Perspective views of both structures are shown in Fig. 10 and 11, with selected bond lengths and angles for comparison.

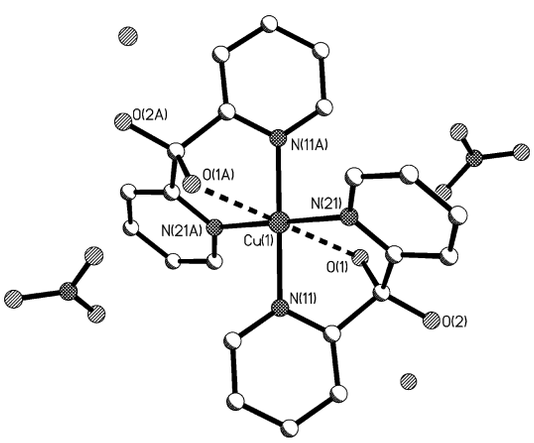


**Fig. 10** A perspective view of the purple coloured form **20**·$2H_2O$. Selected bond lengths (Å) and angles (°): Cu(1)–N(11) 1.992(1), Cu(1)–N(21) 2.048(2), Cu(1)–O(1) 2.477(4); N(11A)–Cu(1)–N(11) 180.0, N(11A)–Cu(1)–N(21) 91.59(7), N(11)–Cu(1)–N(21) 88.41(7), N(11)–Cu(1)–O(1) 73.2(7), N(21)–Cu(1)–O(1) 74.4(7), N(11A)–Cu(1)–O(1) 106.8(9), N(21A)–Cu(1)–O(1) 105.6(9), O(1A)–Cu(1)–O(1) 180.0.

The dihydrate complex, **20**, which has one additional water molecule than **19** in the structure, crystallises in the space group $P2_1/n$ and has previously been reported.[23] It will be briefly described to provide a comparison with the second complex, the monohydrate form, **19**. The asymmetric unit comprises one molecule of **5** in its neutral form, half a copper atom, one

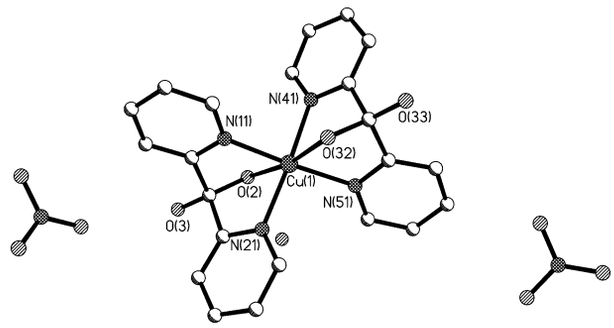


**Fig. 11** A perspective view of the blue coloured form **19**·$H_2O$, with hydrogen atoms omitted for clarity. Selected bond lengths (Å) and angles (°): Cu(1)–N(11) 2.014(2), Cu(1)–N(41) 2.015(2), Cu(1)–N(21) 2.029(2), Cu(1)–N(51) 2.033(2), Cu(1)–O(32) 2.323(2), Cu(1)–O(2) 2.394(2); N(11)–Cu(1)–N(41) 90.15(8), N(11)–Cu(1)–N(21) 87.42(8), N(41)–Cu(1)–N(21) 173.59(8), N(11)–Cu(1)–N(51) 174.38(8), N(41)–Cu(1)–N(51) 87.70(9), N(21)–Cu(1)–N(51) 95.24(8), N(11)–Cu(1)–O(32) 98.19(7), N(41)–Cu(1)–O(32) 75.29(7), N(21)–Cu(1)–O(32) 110.93(8), N(51)–Cu(1)–O(32) 76.25(7), N(11)–Cu(1)–O(2) 75.09(7), N(41)–Cu(1)–O(2) 98.37(7), N(21)–Cu(1)–O(2) 75.27(7), N(51)–Cu(1)–O(2) 110.36(7), O(32)–Cu(1)–O(2) 170.93(7).

nitrate anion and one hydrogen bonded water molecule. The copper atom lies on a centre of inversion and has a distorted octahedral geometry with Jahn–Teller elongation of the weak axial Cu–O bonds. The Cu–N bond lengths of the copper atom in complex **20** are 1.992(1) and 2.048(2) Å, while the Cu–O distance is 2.477(4) Å, which represents a weak bond. An intricate hydrogen-bonding network connects the symmetry-related non-coordinated water molecules and nitrate anions to the complex. These water molecules hydrogen bond to O(2) or O(2A) of the ligand, while the two symmetry-related nitrate anions are hydrogen bonded to O(1) or O(1A). The O ··· O distance for the former two hydrogen bonds is 2.700(8) Å, while for the latter two hydrogen-bonding interactions it is 2.724(8) Å.

The monohydrate complex **19** crystallises in the space group *Cc*, with one full $ML_2$ complex, two non-coordinated nitrate anions and one hydrogen bonded water molecule in the asymmetric unit. The Cu–N bond lengths are fairly similar in both complexes, but by contrast to complex **20**, the Cu–O bond lengths in the blue crystals, complex **19**, are considerably shorter at 2.323(2) and 2.394(2) Å.

In each complex, the nitrate anions and water molecules participate in an intricate hydrogen-bonding network that surrounds the complex, suggesting the possibility of some form of outer-sphere control of the Jahn–Teller distortion in the solid state. Other closely related copper complexes have been described with different anions and solvate molecules that have a range of different bond lengths to the apical hydroxyl groups of ligand **5**.[23,24] These M–O distances range from 2.352 to 2.467 Å.

Unfortunately, we observed no examples of ligand **3** acting as a bridging ligand in coordination complexes. In all examples, it is likely that **3** has undergone decomposition to initially give a mixture of di-2-pyridylketone and **1**, as described above. Di-2-pyridylketone, its hydrated forms and solvolysis products have been well investigated and many reports of the coordination chemistry of these derivatives described. This is because the ketone is activated in the presence of coordinated metal ions[25] and readily forms several solvated derivatives. This decomposition product, **5**, was also observed in the formation of the $M_6L_4$ complex (**11**), described above.

### X-Ray crystallography of complexes of ligand 4

**Structure of $[Cu_2(4)(NO_3)_4] \cdot 4CH_3OH$ (21·$4CH_3OH$).** A crystal structure analysis undertaken on complex **21** revealed the crystals to have almost identical cell dimensions to those obtained for **14**. These two complexes are therefore isomorphous, but not isostructural; the structures differ in the geometry

of the two carbon linker moieties and in the absence of the ethane hydrogen atoms. A perspective view of the structure is shown for comparison in Fig. 12, with the hydrogen atoms and the non-coordinated methanol solvate molecules omitted for clarity. The copper atom has almost identical bond lengths and angles to the previously described copper complex with ligand **2**, and the $\tau$ value for **21** is 0.02, indicating that the coordination geometry is very similar to the previous complex **14**. Due to the greater rigidity of the ligand core and the similar *anti* arrangement of the metal atoms, the metal–metal distance between the two copper atoms is 7.094(1) Å, which is longer than the corresponding distance for **14** (6.698(1) Å).

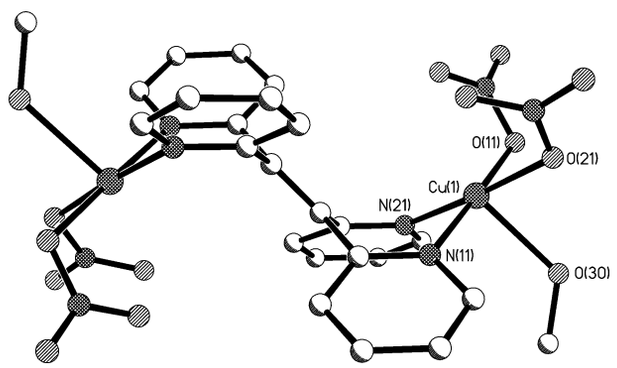


**Fig. 12** A perspective view of **21** with the hydrogen atoms and the non-coordinated methanol solvate molecules omitted for clarity. Selected bond lengths (Å) and angles (°): Cu(1)–O(21) 1.978(6), Cu(1)–N(21) 1.977(7), Cu(1)–O(11) 1.995(6), Cu(1)–N(11) 2.003(7), Cu(1)–O(30) 2.271(6); O(21)–Cu(1)–N(21) 176.3(3), O(21)–Cu(1)–O(11) 88.3(3), N(21)–Cu(1)–O(11) 89.7(3), O(21)–Cu(1)–N(11) 93.7(3), N(21)–Cu(1)–N(11) 88.3(3), O(11)–Cu(1)–N(11) 178.0(3), O(21)–Cu(1)–O(30) 82.9(2), N(21)–Cu(1)–O(30) 99.9(3), O(11)–Cu(1)–O(30) 85.3(2), N(11)–Cu(1)–O(30) 95.5(3).

A related dinuclear copper perchlorate complex of this ligand has been reported with a hydroxide ligand also bridging the two copper atoms.[11] This was prepared, as noted earlier, by reaction of copper perchlorate, **1** and di-2-pyridylketone. The Cu–Cu distance (3.663(3) Å) is considerably shorter than that in **21** because of the $\mu_2$-hydroxide bridge between the copper centres, which enforces a *syn* arrangement of the two copper centres.

**Structure of $[Pd_2(4)(OAc)_4]\cdot 6H_2O$ (23).** Complex **23** is also a dinuclear complex of ligand **4**, as suggested by elemental analysis. It crystallises in the monoclinic space group *C*2/*c*, with four molecules in the unit cell. The asymmetric unit contains one palladium atom, half the ligand, two coordinated acetate anions and three water molecules. A perspective view of the structure is shown in Fig. 13. As expected the palladium centre is square planar, with bond distances typical for such complexes. The Pd–N and Pd–O bond lengths are between 2.015(4) and 2.028(4) Å. The Pd–Pd distance is 7.002(1) Å, consistent with other complexes bridged only by this ligand.

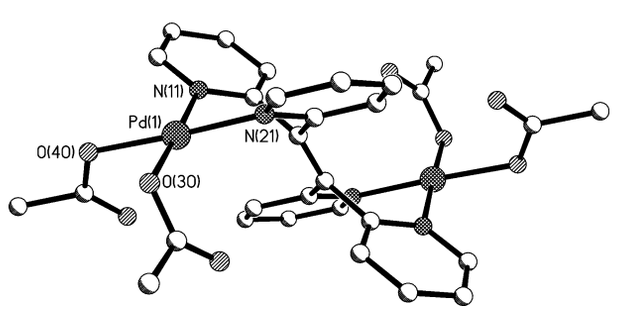


**Fig. 13** A perspective view of complex **23**, with hydrogen atoms and solvated water omitted for clarity. Selected bond lengths (Å) and angles (°): Pd(1)–O(30) 2.016(4), Pd(1)–N(21) 2.017(4), Pd(1)–N(11) 2.024(4), Pd(1)–O(40) 2.028(4); O(30)–Pd(1)–N(21) 91.20(15), O(30)–Pd(1)–N(11) 178.14(14), N(21)–Pd(1)–N(11) 89.70(15), O(30)–Pd(1)–O(40) 87.45(14), N(21)–Pd(1)–O(40) 176.61(13), N(11)–Pd(1)–O(40) 91.57(14).

Like the other complexes of ligand **4**, the ethene bridge is planar, and the pyridine rings of the ligand twist significantly out of the plane of the ethene backbone to coordinate and minimise steric hindrance between the H3 protons of the pyridine rings. When viewed down the crystallographic *c*-axis the discrete complexes stack one-on-top-another, and the water solvate molecules and acetate anions participate in an intricate hydrogen-bonding network within the columnar channels formed by molecules of the complex. Specifically, six water solvate molecules form a cyclic hexagonal, hydrogen-bonded ring within this column. This interesting 'ring of ice'[26] connects to the complex *via* hydrogen bonds with the oxygen atoms of the acetate anions.

**Structure of $[Zn_2(4)(OAc)_4(H_2O)_2]$ (24).** The structure of complex **24** was determined using X-ray crystallography, and confirmed that this complex was also dinuclear, with the ligand chelating to two zinc atoms. The asymmetric unit contains one zinc atom, one half of the bridging ligand molecule, two acetate counterions and a coordinated water molecule. A perspective view of the complex, which crystallises in the triclinic space group $P\bar{1}$, is shown in Fig. 14 with the hydrogen atoms removed for clarity. The geometry about the zinc atoms is highly distorted trigonal-bipyramidal ($\tau$ value = 0.58), with one pyridine ring and the coordinated water molecule occupying the axial positions in the primary coordination sphere. Molecules of the discrete coordination complex are linked through two intermolecular hydrogen bonds between the coordinated water molecule and an acetate anion in an adjacent complex. The Zn–Zn distance is 7.354(1) Å, which is slightly longer than in other dinuclear complexes of this ligand, and considerably longer than in complex **16** (6.571(1) Å), which is bridged by ligand **2**.

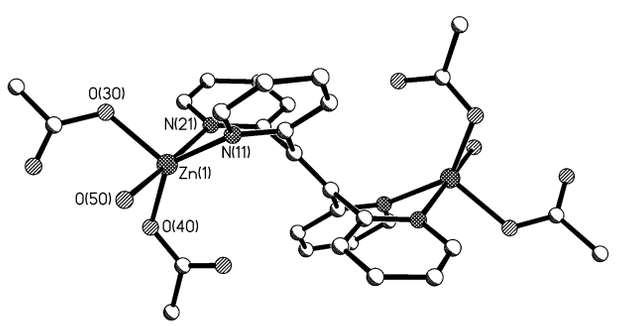


**Fig. 14** A perspective view of complex **24**, formed from reaction of zinc acetate with **4**. Hydrogen atoms are omitted for clarity. Selected bond lengths (Å) and angles (°): Zn(1)–O(40) 1.980(2), Zn(1)–O(30) 1.990(2), Zn(1)–N(11) 2.093(2), Zn(1)–O(50) 2.152(2), Zn(1)–N(21) 2.210(2); O(40)–Zn(1)–O(30) 106.10(7), O(40)–Zn(1)–N(11) 139.17(7), O(30)–Zn(1)–N(11) 114.63(7), O(40)–Zn(1)–O(50) 92.98(7), O(30)–Zn(1)–O(50) 90.63(6), N(11)–Zn(1)–O(50) 89.46(6), O(40)–Zn(1)–N(21) 93.12(7), O(30)–Zn(1)–N(21) 88.85(6), N(11)–Zn(1)–N(21) 85.12(6), O(50)–Zn(1)–N(21) 173.78(6).

## Discussion

This study of the coordination chemistry of the bridging ligands **2**, **3** and **4**, and the model compound **1**, has revealed a number of different coordination modes and structural features. A commonly observed structure was a discrete dinuclear complex, but a coordination polymer and a [2 + 2]-dimetallomacrocycle were characterised for **2**. The coordination chemistry of ligands **2** and **4** is very similar, with only slight differences in the metal–metal distances, which originate because of the extra rigidity of the conjugated bridge between the chelating units in ligand **4**. The metal–metal distances range

from 6.571–6.835 Å for complexes of **2** whereas complexes of **4** have metal–metal distances ranging from 7.002–7.354 Å.

In all examples where complexes were structurally characterised, ligands **2** and **4** bridge two metal centres, with only one case (complex **13**) where the ligand is hypodentate. In no case was a complex characterised where a 7-membered chelate ring forms in preference to the more favoured 6-membered ring. These results are in distinct contrast to the ruthenium chemistry of these ligands previously reported by us.[10] In bis(2,2′-bipyridine)ruthenium(II) complexes these ligands proved extremely resistant to the formation of dinuclear complexes despite extensive efforts to effect such reactions. Both **2** and **4** are considerably more stable than ligand **3**, which was not reacted without undergoing some form of decomposition.

Recently, the metal complexes of a related ligand system have been studied where the ligands are based around the 4,5-diazafluorene ring system[27] in place of the di-2-pyridylmethane building block incorporated in the ligands investigated here. These ligands, 9,9′-bis(4,5-diazafluorenyl) (**25**) and 9,9′-bis(4,5-diazafluorenylidene) (**26**) have what are effectively 3-substituted pyridine rings that have been bonded through the 2-position to create a planar chelating domain (see Fig. 15). Transition metal complexes of **25** and **26** have been described with ruthenium(II), cobalt(II), nickel(II) and zinc(II).[27] It appears that the reduced flexibility of these ligands have thus far prevented the crystallisation of such complexes for study by X-ray crystallography. However, it is worth noting some interesting differences, in addition to the changes in flexibility of the chelating unit, between the two sets of ligands. Ligands **2** and **4** have the potential to form 6- or 7-membered chelate rings, although the former is more likely, whereas the diazafluorene-based ligands will form 5-membered rings on chelation to metal centres. The bite angle in the two sets of ligands is also considerably different, with the 5-membered ring in the 4,5-diazafluorene system responsible for a significant widening of the bite angle of **25** and **26**.

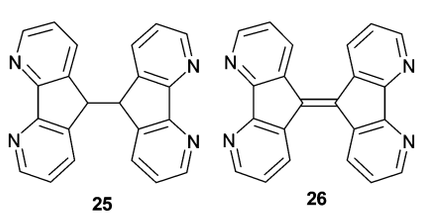


**25** **26**

**Fig. 15** The structures of ligands **25** and **26** with 4,5-diazafluorene subunits.

## Conclusions

In summary, we have described the synthesis and study of the transition metal complexes of three closely related bridging ligands and the simple model chelating unit, **1**. Ligand **1** was shown to adopt a novel bridging coordination mode in complexes **7** and **17**, while no complexes of **3** could be isolated where the ligand remained intact. The effect of oxidising the carbon backbone of ligand **2**, with the concomitant loss of flexibility and extension of the conjugation in **4**, does not significantly change the coordination chemistry of these ligands. The potential utility of the two bridging ligands, **2** and **4**, in the field of metallosupramolecular chemistry was demonstrated when **2** was reacted with different silver salts to produce both a coordination polymer and a [2 + 2] molecular box structure.

## References


1 A. Juris, V. Balzani, F. Barigelletti, S. Campagna, P. Belser and A. von Zelewsky, *Coord. Chem. Rev.*, 1988, **84**, 85; P. J. Steel, *Coord. Chem. Rev.*, 1990, **106**, 227; C. Richardson, P. J. Steel, D. M. D'Alessandro, P. C. Junk and F. R. Keene, *J. Chem. Soc., Dalton Trans.*, 2002, 2775.

2 V. Balzani, A. Juris, M. Venturi, S. Campagna and S. Serroni, *Chem. Rev.*, 1996, **96**, 759.

3 C. Kaes, A. Katz and M. W. Hosseini, *Chem. Rev.*, 2000, **100**, 3553.

4 M. Munakata, L. P. Wu and T. Kuroda-Sowa, *Adv. Inorg. Chem.*, 1999, **46**, 173; B. Moulton and M. J. Zaworotko, *Chem. Rev.*, 2001, **101**, 1629; M. J. Zaworotko, *Chem. Commun.*, 2001, 1; J. A. R. Navarro and B. Lippert, *Coord. Chem. Rev.*, 2001, **222**, 219; M. Fujita, K. Umemoto, M. Yoshizawa, N. Fujita, T. Kusukawa and K. Biradha, *Chem. Commun.*, 2001, 509; C. J. Jones, *Chem. Soc. Rev.*, 1998, **27**, 289; S. Leininger, B. Olenyuk and P. J. Stang, *Chem. Rev.*, 2000, **100**, 853; G. F. Sweigers and T. J. Malefetse, *Chem. Rev.*, 2000, **100**, 3483; G. F. Sweigers and T. J. Malefetse, *Chem. Eur. J.*, 2001, **7**, 3637; S. R. Batten and R. Robson, *Angew. Chem., Int. Ed.*, 1998, **37**, 1460; B. J. Holliday and C. A. Mirkin, *Angew. Chem., Int. Ed.*, 2001, **40**, 2022; R. Robson, *J. Chem. Soc., Dalton Trans.*, 2000, 3735.

5 F. R. Keene, *Coord. Chem. Rev.*, 1997, **166**, 121; V. Balzani, A. Credi, F. M. Raymo and J. F. Stoddart, *Angew. Chem., Int. Ed.*, 2000, **39**, 3348; E. C. Constable, *Chem. Commun.*, 1997, 1073; V. Balzani, S. Campagna, G. Denti, A. Juris, S. Serroni and M. Venturi, *Acc. Chem. Res.*, 1998, **31**, 26; L. Sun, L. Hammarstrom, B. Akermark and S. Styring, *Chem. Soc. Rev.*, 2001, **30**, 36; M. Yagi and M. Kaneko, *Chem. Rev.*, 2001, **101**, 21.

6 E. C. Constable and P. J. Steel, *Coord. Chem. Rev.*, 1989, **93**, 205.

7 A. J. Canty and N. J. Minchin, *Aust. J. Chem.*, 1986, **39**, 1063.

8 A. J. Canty, N. Chaichit, B. M. Gatehouse, E. E. George and G. Hayhurst, *Inorg. Chem.*, 1981, **20**, 2414; E. Spodine, J. Manzur, M. T. Garland, J. P. Fackler, Jr., R. J. Staples and B. Trzcinska-Bancroft, *Inorg. Chim. Acta*, 1993, **203**, 73.

9 A. J. Canty and N. J. Minchin, *Inorg. Chim. Acta*, 1985, **100**, L13.

10 D. M. D'Alessandro, F. R. Keene, P. J. Steel and C. J. Sumby, *Aust. J. Chem.*, 2003, **56**, 657.

11 E. Spodine, J. Manzur, M. T. Garland, M. Kiwi, O. Pena, D. Grandjean and L. Toupet, *J. Chem. Soc., Dalton Trans.*, 1991, 365.

12 J. Manzur, M. T. Garland, A. M. Atria, M. Vera and E. Spodine, *Bol. Soc. Chil. Quim.*, 1989, **34**, 229.

13 G. M. Sheldrick, SADABS, University of Göttingen, Germany, 1998.

14 G. M. Sheldrick, *Acta Crystallogr., Sect. A*, 1990, **46**, 467.

15 G. M. Sheldrick, SHELXL-97, University of Göttingen, Germany, 1997.

16 M. Melnik, M. Kabesova, M. Koman, L. Macaskova, J. Garaj, C. E. Holloway and A. Valent, *J. Coord. Chem.*, 1998, **45**, 147.

17 A. W. Addison, T. N. Rao, J. Reedijk, J. Van Rijn and G. C. Verschoor, *J. Chem. Soc., Dalton Trans.*, 1984, 1349.

18 C. Tsiamis, A. G. Hatzidimitiou and L. Tzavellas, *Inorg. Chem.*, 1998, **37**, 2903.

19 C. Hemmert, M. Renz, H. Gornitzka, S. Soulet and B. Meunier, *Chem. Eur. J.*, 1999, **5**, 1766.

20 V. Tangoulis, C. P. Raptopoulou, S. Paschalidou, A. E. Tsohos, E. G. Bakalbassis, A. Terzis and S. P. Perlepes, *Inorg. Chem.*, 1997, **36**, 5270; Z. E. Serna, R. Cortes, M. K. Urtiaga, M. G. Barandika, L. Lezama, M. I. Arriortua and T. Rojo, *Eur. J. Inorg. Chem.*, 2001, 865; C. A. Kavounis, C. Tsiamis, C. J. Cardin and Y. Zubavichus, *Polyhedron*, 1996, **15**, 385.

21 E. Katsoulakou, N. Lalioti, C. P. Raptopoulou, A. Terzis, E. Manessi-Zoupa and S. P. Perlepes, *Inorg. Chem. Commun.*, 2002, **5**, 719.

22 B. Milani, G. Mestroni and E. Zangrando, *Croat. Chim. Acta*, 2001, **74**, 851.

23 S.-L. Wang, J. W. Richardson, S. J. Briggs, R. A. Jacobson and W. P. Jensen, *Inorg. Chim. Acta*, 1986, **111**, 67.

24 V. Tangoulis, C. P. Raptopoulou, A. Terzis, S. Paschalidou, S. P. Perlepes and E. G. Bakalbassis, *Inorg. Chem.*, 1997, **36**, 3996; G. Yang, M.-L. Tong, X. M. Chen and S. W. Ng, *Acta Crystallogr., Sect. C*, 1998, **54**, 732; Z. Serna, M. G. Barandika, R. Cortes, M. K. Urtiaga and M. I. Arriortua, *Polyhedron*, 1999, **18**, 249; S. R. Breeze, S. Wang, J. E. Greedan and N. P. Raju, *Inorg. Chem.*, 1996, **35**, 6944; O. J. Parker, S. L. Aubol and G. L. Breneman, *Polyhedron*, 2000, **19**, 623.

25 A. J. Canty, P. R. Traill, B. W. Skelton and A. H. White, *Inorg. Chim. Acta*, 1997, **255**, 117.

26 R. Custelcean, C. Afloroaei, M. Vlassa and M. Polverejan, *Angew. Chem., Int. Ed.*, 2000, **39**, 3094; R. Ludwig, *Angew. Chem., Int. Ed.*, 2001, **40**, 1808; F. N. Keutsch, J. D. Cruzan and R. J. Saykally, *Chem. Rev.*, 2003, **103**, 2533.

27 M. Riklin and A. Von Zelewsky, *Helv. Chim. Acta*, 1996, **79**, 2176; M. Riklin, A. Von Zelewsky, A. Bashall, M. McPartlin, A. Baysal, J. A. Connor and J. D. Wallis, *Helv. Chim. Acta*, 1999, **82**, 1666; A. Baysal, J. A. Connor and J. D. Wallis, *J. Coord. Chem.*, 2001, **53**, 347.